

SPECTROPHOTOMETRIC DETERMINATION OF REACTION STOICHIOMETRY AND EQUILIBRIUM CONSTANTS OF METALLOCHROMIC INDICATORS. III. ANTIPYRYLAZO III COMPLEXING WITH Ca^{2+} AND ACETYLCHOLINE RECEPTOR PROTEIN

Peter L. DOROGI, Karen MOSS, Eberhard NEUMANN *

Max-Planck-Institut für Biochemie, D-8033 Martinsried/München, F.R.G.

and

Hai Won CHANG

Department of Neurology, College of Physicians and Surgeons, Columbia University, New York, NY 10032, U.S.A.

Received 3 March 1981

Revised manuscript received 30 March 1981

Stoichiometries, equilibrium constants and optical extinction coefficients of calcium–antipyrylazo III (An) complexing are determined with the analytical method described in article I of this series. Spectrophotometric Ca titrations of An at the wavelengths 595 and 710 nm indicate overall dissociation equilibrium constants for the complexes CaAn , CaAn_2 and Ca_2An to be $4.5 \times 10^{-4} \text{ M}$, $1.1 \times 10^{-8} \text{ M}^2$ and $1.5 \times 10^{-6} \text{ M}^2$, respectively, extrapolated to zero ionic strength. Ca titrations of solutions containing An plus acetylcholine receptor protein give clear evidence that An binds to the protein to a large extent in the presence of Ca^{2+} ; furthermore, addition of acetylcholine results in release of protein-bound Ca and An. This is the first reported indication that antipyrylazo III binds to biological material and questions the usefulness of this dye as a Ca indicator in biological systems.

1. Introduction

A new analytical method was recently described which resolves multiple metal-ion binding characteristics of metallochromic indicators, as well as optical extinction coefficients of the resultant metal-indicator complexes. Theoretical details are given in article I [1] of this series, and application of the method to determine Ca^{2+} -binding properties of the high-affinity indicator arsenazo III are described in article II [2]. In this report, the method is applied to determine Ca complexing with antipyrylazo III (An), a so-called ‘middle-range’ Ca^{2+} -affinity indicator ($K_{\text{Ca}} \approx 10^{-5} \text{ M}$).

An has been used to study Ca^{2+} transport kinet-

ics in mitochondria, sarcoplasmic reticulum and chromaffin vesicles, among others [3,4], and for the measurement of cytosolic Ca^{2+} concentrations (cf. ref [4]). Important advantages of An over the more widely used indicator arsenazo III are its total selectivity for Ca^{2+} over Mg^{2+} at wavelengths greater than 660 nm (Ca^{2+} effects being maximal at 710 nm), and the Ca^{2+} sensitivity of An near the red end of the visible spectrum, allowing measurement of free-Ca concentration ($[\text{Ca}]$) in the presence of biological chromophores. In addition, the time constant for Ca^{2+} -dye complexing is about an order of magnitude smaller for An than for arsenazo III, which renders An more suitable for kinetic resolution of rapid changes in $[\text{Ca}]$.

Calibration of indicator absorbance changes in terms of $[\text{Ca}]$ is difficult if more than one type of

* To whom correspondence should be addressed.

Ca-dye complex is present. Consequently, applicability of indicators has in the past been deemed reliable only in [Ca] ranges where absorbance changes linearly with Ca concentration. However, because in the case of antipyrilazo III this limitation would restrict its use to Ca levels below 100 characterization of Ca-binding properties of many proteins. For example, spectrophotometric studies of acetylcholine receptor protein isolated from *Torpedo* fish, using murexide as indicator, show the presence of Ca-binding sites extending from the μM to the mM range [5,6]. The main calibration difficulty is that, in general, the total absorbance depends not only on the total amount of Ca^{2+} which is bound to indicator, but also on the distribution of Ca^{2+} and dye among different complexes, each with possibly different absorbance characteristics. When several types of complexes are present, the measured absorbance is a reflection of more than one thermodynamic binding and optical parameter, and these parameters are not resolvable from conventional calibration methods, e.g., Scatchard plots.

We outline below how the analysis described in articles I and II resolves Ca-An complexing properties; there is appreciable mixing of two stoichiometric types even at the lowest practical concentrations. A third type of complex dominates when $[\text{Ca}] \geq 10^{-3} \text{ M}$. Binding stoichiometries and corresponding equilibrium constants were determined from Ca titrations performed at two practical wavelengths, 595 and 710 nm.

It has been reported previously that An does not bind to cells or cell organelles [3]; in contrast, we find that the dye binds to acetylcholine receptor protein in the presence of Ca.

2. Materials and methods

2.1. Purification of indicator

An (280 mg; a product of ICN Pharmaceuticals) was dissolved in 3 ml of H_2O plus 3 ml of solution I, which contained *n*-butanol, pyridine, acetic acid and H_2O in the volume ratio 15:10:3:12. The resulting solution was passed through a 2.5 cm \times 35 cm column filled with

Whatman DE52 DEAE-cellulose, preswollen in solution I. The first of at least four differently colored fractions contained the dye. After evaporation, the dye powder was dissolved in 30 ml H_2O and any remaining Ca^{2+} was removed by applying the solution to a 1.5 cm \times 20 cm ion-exchange column containing the Na form of Chelex 100 (Biorad Labs). The eluate was lyophilized, and the powder was dissolved in 5 ml of H_2O plus a few droplets of concentrated HCl. After 12 h at 4°C, An precipitates and can be collected by filtration and vacuum drying. Further details of the method have been given by Kendrick [7]. By atomic absorption spectroscopy, the final yield of 190 mg dye contained < 0.003 mole of Ca^{2+} per mole of An.

2.2. Protein isolation and purification

Purification of acetylcholine receptor protein followed the method described by Chang and Bock [8,9], which yields purified protein with a minimal degree of delipidation. Initially frozen electric organ tissue from *Torpedo marmorata* and *Torpedo californica* (500 g) was quickly thawed by homogenization with a 1 l solution containing 20 mM *N*-2-hydroxyethylpiperazine-*N'*-2-ethanesulfonic acid (Hepes buffer, pH 7.0, 293 K), 0.02% sodium azide, 5 mM *N*-ethylmaleimide and 0.1 mM phenylmethanesulfonyl fluoride (PMSF, from Sigma). After centrifugation, the pellet was suspended in a 200 ml solution containing 1.2% Lubrol WX (Sigma) and 0.1 mM PMSF, and was shaken for 4 h at 4°C. A 50 mM CaCl_2 solution was added dropwise with continuous mixing until $[\text{Ca}] = 1 \text{ mM}$ was reached. The suspension was centrifuged at 46000 g for 1 h, yielding a protein-rich supernatant.

The crude extract was applied to a Sepharose 4B column (2.4 cm \times 22 cm) pretreated with the affinity ligand methyl-(*N*-(6-aminocaproyl)-6'-aminocaproyl)-3-amino)pyridinium bromide hydrobromide (Dicaproyl-MP). The column was first washed with the buffer solution to remove contaminating proteins and the receptor protein was eluted using stock buffer containing 1 mM CaCl_2 , 25 mM NaCl and 70 μM gallamine triethiodide (Flaxedil, from K&K Labs). Protein was con-

centrated by vacuum dialysis under N_2 using a collodion membrane bag (Schleicher and Schüll). The final protein solution contained 1–2 mg protein (plus endogenous lipids) per ml, 0.1 M Hepes buffer, 0.1 M NaCl, 0.01 mM $CaCl_2$ and 0.01% Lubrol WX; pH 7.0 at 293 K.

2.3. Calcium titrations

Absorbance spectra and Ca titrations were performed at 293 K in a thermostatically controlled cell with a Cary 118C spectrophotometer (see ref. [2]). All vessels were washed with 1 μ M EDTA and then rinsed with deionized (multiply reflux-distilled) water which had a conductivity of 0.9 μ S cm^{-1} . The buffer of the Ca titrations of the indicator and of the protein-indicator solution at the Ca-specific wavelength 710 nm is 0.1 M NaCl, 0.1 M Hepes, pH 7.0 at 293 K; the initial ionic strength of the indicator solution is $I_c = 0.2$ M. The Ca titrations of An at 595 nm were performed in 0.05 M piperazine- N,N' -bis(2-ethanesulfonic acid) (Pipes buffer), pH 7.0 at 293 K; the initial ionic strength is $I_c = 0.05$ M. At pH 6.5–7.5 the absorbance of An is found to be independent of pH, and the contribution of Na^+ -indicator complexes to the absorbance at $[Na] \leq 0.1$ M is negligibly small.

3. Optical and thermodynamic constants

3.1. Absorbance spectra and extinction coefficients of antipyrilazo III

Fig. 1 shows a section of the difference absorption spectra recorded for several An-Ca solutions, differing in total Ca concentration. There are no isosbestic wavelengths, which suggests multiple types of Ca-indicator complexing. The complexes evidently differ in overall stability with respect to Ca^{2+} concentration.

Accurate determination of the extinction coefficient of Ca^{2+} -free indicator (ϵ_{An}) is less complicated by cation contamination from buffer and indicator salts than was previously found for arsenazo III [2]. ϵ_{An} can be estimated from a graphical extrapolation procedure described in refs.

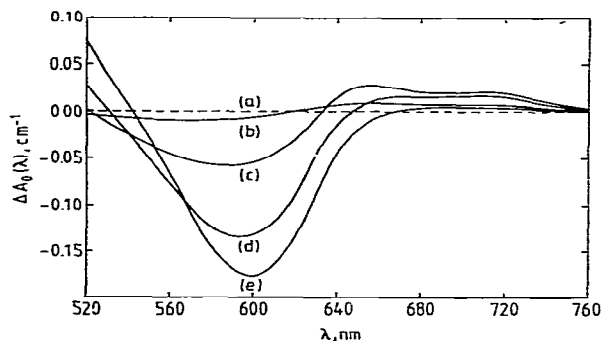


Fig. 1. Difference spectra (section) of An, $\Delta A_0(\lambda)$, defined by eq. (1) of text; 0.05 M pipes buffer, pH 7.0 at 293 K; $[An_T] = 8.49 \times 10^{-6}$ M: (a) $[Ca_T] \approx 0$, 2 mM EDTA, (b) $[Ca_T] = 8.5 \times 10^{-5}$ M, (c) 8.5×10^{-4} M, (d) 8.5×10^{-3} M, (e) 8.5×10^{-2} M. No isosbestic points are apparent.

[1,2]; it was found that $\epsilon_{An} = 2.61 \times 10^4$ cm^{-1} M^{-1} at 595 nm and $\epsilon_{An} = 0.3 \times 10^3$ cm^{-1} M^{-1} at 710 nm.

3.2. Calcium titrations of antipyrilazo III

Figs. 2a and b show changes in absorbance per cm, ΔA_0 , at 595 and 710 nm, respectively, for a variety of total indicator concentrations ($[An_T]$) as total Ca concentration ($[Ca_T]$) is varied. For data plots ΔA_0 is defined by

$$\Delta A_0 = A v / v_0 - \epsilon_{An} [An_T]_0 \quad (1)$$

where A is the total measured absorbance corresponding to a given titration point, and $[An_T]_0$ is the total indicator concentration at the initial sample volume v_0 [1,2]. On the other hand, for data analysis with the various expressions described below, ΔA is defined more generally by

$$\Delta A = A - \epsilon_{An} [An_T] \quad (2)$$

In part b of fig. 2 it is seen that the absorbance change ΔA_0 first rises with increasing $[Ca_T]$, but then decreases, and approaches the absorbance of the Ca-free indicator. This behavior at 710 nm reflects the formation of *at least* two optically different Ca-An complexes, and corroborates the inferences already derived from the lack of isosbestic wavelengths in fig. 1.

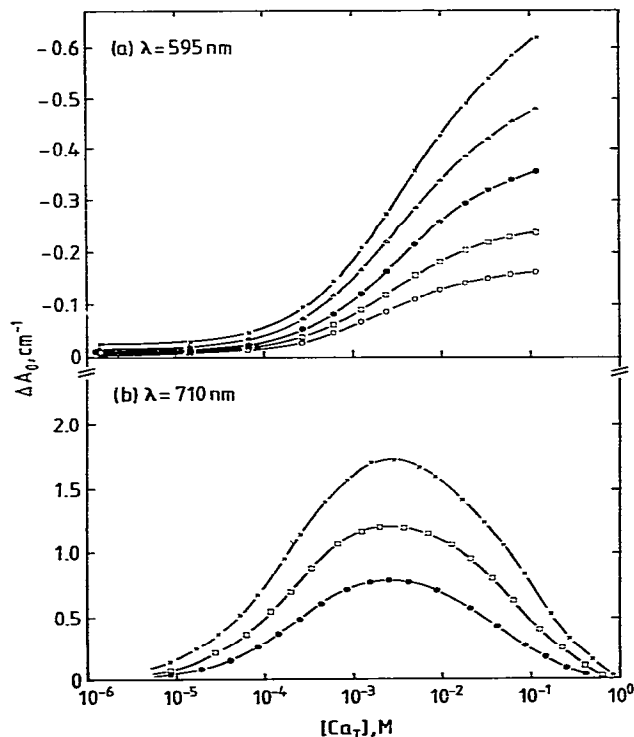


Fig. 2. Absorbance changes of An, ΔA_0 [defined by eq. (1)], as a function of total Ca concentration, $[Ca_T]$, at 293 K. for (a) $\lambda = 595$ nm, 0.05 M Pipes, pH 7.0; total indicator concentrations are $[An_T] = 7.5 \times 10^{-6}$ M (open circles), 1.11×10^{-5} M (open squares), 1.65×10^{-5} M (solid circles), 2.25×10^{-5} M (open triangles) and 2.95×10^{-5} M (crosses); (b) $\lambda = 710$ nm, 0.1 M NaCl, 0.1 M Hepes, pH 7.0; $[An_T] = 1.0 \times 10^{-4}$ M (solid circles), 1.5×10^{-4} M (open squares) and 2.0×10^{-4} M (crosses).

3.3 Analysis of calcium-antipyrilazo III complexing

When Ca complexes with indicator in only one stoichiometric form, Ca_pAn_q , mass conservation constraints on Ca and dye reduce the expression for the overall thermodynamic dissociation equilibrium constant K'_{pq} of the reaction



to the following form [1]:

$$\begin{aligned} K'_{pq} &= \{[Ca]^p [An]^q / [Ca_pAn_q]\} \Pi f'_{pq} \\ &= \{[Ca_T] - p \Delta A / q \Delta \epsilon_{pq}\}^p \\ &\quad \times \{[An_T] - \Delta A / \Delta \epsilon_{pq}\}^q \Pi f'_{pq} \\ &\quad \times \{\Delta A / q \Delta \epsilon_{pq}\}^{-1}. \end{aligned} \quad (4)$$

In eq. (4), $[Ca]$ and $[An]$ are the concentrations of free (uncomplexed) Ca and An, respectively, and $\Delta \epsilon_{pq}$ is defined as the difference of molar extinction coefficients,

$$\Delta \epsilon_{pq} = \epsilon_{pq} / q - \epsilon_{An}; \quad (5)$$

ϵ_{pq} is the extinction coefficient of the complex Ca_pAn_q . The overall activity coefficient product $\Pi f'_{pq} = (f_{Ca})^p (f_{An})^q / f_{Ca_pAn_q}$ adjusts the apparent dissociation equilibrium constant to zero ionic strength. The $\Pi f'_{pq}$ values are calculated according to the Debye-Hückel approximation described in article I; however, because the buffer ionic strength was in each case at least 0.05 M, the $\Pi f'_{pq}$ values are essentially invariant with changing $[Ca_T]$ in the range where $[Ca_T] \ll 0.05$ M. The charge number of An at pH 7.0 was taken as -2 , reflecting ionization of the two HSO_3 groups. Diminution of $\Pi f'_{11}$ for $p = q = 1$, i.e., $Ca^{2+} + An^{2-} = CaAn^0$, with increasing ionic strength is shown in fig. 3: $\Pi f'_{11} = \Pi f_{11} = 0.22$ at an ionic strength of $I_c = 0.05$ M and at 293 K. The absence of the prime notation on K_{pq} and Πf_{pq} indicates reference to

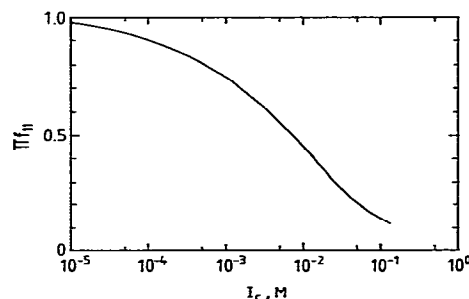


Fig. 3. Activity coefficient product Πf_{11} as a function of ionic strength, I_c , for the reaction $Ca^{2+} + An^{2-} = CaAn^0$; see eq. (A.2) of ref. [1]. At 293 K, with the 'distance of closest approach' taken as 5.0×10^{-8} cm, $\log \Pi f_{11} = \{(-8)(0.507 \text{ M}^{-1/2}) \times I_c^{1/2}\} / \{1 + [(0.328 \times 10^8 \text{ cm}^{-1} \text{ M}^{-1/2})(5.0 \times 10^{-8} \text{ cm}) I_c^{1/2}]\} + (0.2)I_c$; $\Pi f'_{12} \approx \Pi f'_{21} \approx \Pi f_{11}$ (see text).

elementary, rather than overall, complexing reactions. In parts I and II of this series, the $\Pi f'_{pq}$ terms were formally not explicitly included in the expressions for K'_{pq} ; the calculations, however, used the constancy of the thermodynamic equilibrium constants.

If the assumption that only one stoichiometric form Ca_pAn_q exists is correct, then there must also exist a unique combination of parameters p , q and $\Delta\epsilon_{pq}$ for which the right-hand side of eq. (4) has the same numerical value of *each* experimental data set ($[\text{Ca}_T]$, $[\text{An}_T]$, ΔA). This condition is the crucial test of the 'one-complex' assumption, because thermodynamic dissociation constants are, by definition, independent of concentrations.

Because An is a relatively small molecule, and its net charge number is -2 , the stoichiometric integers p and q are expected to be either 1 or 2. Furthermore, the plausible range of values to be scanned for $\Delta\epsilon_{pq}$ is suggested by the magnitude of $\Delta A/[\text{An}_T]$.

It was found that even the low- $[\text{Ca}_T]$ part of the ΔA data could not be covered with a single-complex formalism; the absorbance values are incompatible with the desired $[\text{Ca}_T]$ and $[\text{An}_T]$ independence of K'_{pq} as defined in eq. (4). This result is clear evidence that the one-complex model is an incorrect oversimplification of the Ca-An interaction. In practice, the one-complex model is expected to apply only when $p=q=1$, because lower-order complexes are also expected to be present when p or q is >1 ; exceptions to this rule are the case of extremely strong positive cooperative binding, or when all binding sites are saturated (high $[\text{Ca}_T]$).

The low- $[\text{Ca}_T]$ titration points for the Ca-An interaction indicate the presence of at least two distinct stoichiometric types, CaAn and CaAn_2 . This result was obtained with an 'equilibrium-constant constancy test', similar to eq. (4), but incorporating *two* types of complexes. Fundamental relations are the law of additive absorptivities,

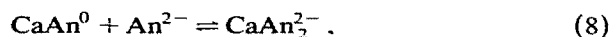
$$\Delta A = \Delta\epsilon_{11}[\text{CaAn}] + q\Delta\epsilon_{pq}[\text{Ca}_p\text{An}_q], \quad (6)$$

and mass conservation laws:

$$[\text{An}_T] = [\text{An}] + [\text{CaAn}] + q[\text{Ca}_p\text{An}_q], \quad (7a)$$

$$[\text{Ca}_T] = [\text{Ca}] + [\text{CaAn}] + p[\text{Ca}_p\text{An}_q]. \quad (7b)$$

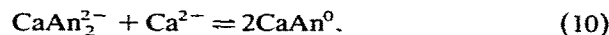
Verification of this model was based on the finding of a constant value for K_{12} , the elementary thermodynamic equilibrium constant of the reaction



from the low- $[\text{Ca}_T]$ titration points. From ref. [1],

$$\begin{aligned} K_{12} &= \frac{[\text{CaAn}][\text{An}]\Pi f_{11}}{[\text{CaAn}_2]} \\ &= \frac{2\Delta\epsilon_{12}[\text{Ca}][\text{An}]^2\Pi f_{12}}{\Delta A K_{11} - [\text{Ca}][\text{An}]\Delta\epsilon_{11}}. \end{aligned} \quad (9)$$

The values of $[\text{Ca}]$ and $[\text{An}]$ are determined by the experimental quantities $[\text{Ca}_T]$, $[\text{An}_T]$ and ΔA , and by the values of the three unknown parameters $\Delta\epsilon_{11}$, $\Delta\epsilon_{12}$ and K_{11} . Although it may at first be thought that trial-and-error computation using three parameters, as in eq. (9), is not an effective method for determining the true stoichiometric distribution, the data analysis showed that only the CaAn - CaAn_2 model was consistent with the thermodynamic requirements. Results of the analysis of titration curves at 595 nm are shown in fig. 4: the large deviation from the desired horizontal trend for K_{12} as $[\text{Ca}_T]$ was raised above 1×10^{-4} M suggests a sharply decreased contribution of CaAn_2 to ΔA at higher Ca concentrations. The disappearance of CaAn_2 is most likely due to the disproportionation reaction



The only choice of extinction coefficients for which constancy of K_{12} was obtained for the low- $[\text{Ca}_T]$ points was

$$\Delta\epsilon_{11} = -5.0 \times 10^3 \text{ cm}^{-1} \text{ M}^{-1},$$

$$\Delta\epsilon_{12} = -5.5 \times 10^3 \text{ cm}^{-1} \text{ M}^{-1} \quad (\text{at } 595 \text{ nm}),$$

and $K_{11} = [\text{Ca}][\text{An}]\Pi f_{11}/[\text{CaAn}] = 4.5 \times 10^{-4}$ M at zero ionic strength. K_{12} is indicated to be $\approx 2.5 \times 10^{-5}$ M (cf. fig. 4), resulting in the overall dissociation equilibrium constant of the CaAn_2 complex

$$\begin{aligned} K'_{12} &= K_{11}K_{12} = (4.5 \times 10^{-4} \text{ M})(2.5 \times 10^{-5} \text{ M}) \\ &= 1.1 \times 10^{-8} \text{ M}^2. \end{aligned}$$

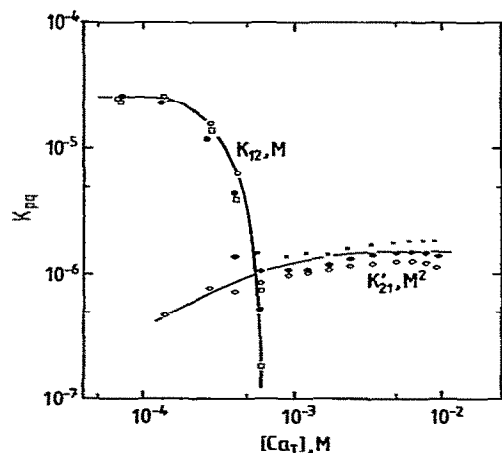


Fig. 4. Estimation of thermodynamic equilibrium constants K_{12} and K'_{21} , as a function of total Ca concentration, according to eqs. (9) and (15), respectively, from ΔA data at 595 nm (fig. 2a). For K_{12} estimation, $[An_T] = 1.65 \times 10^{-5}$ M (solid circles), 2.25×10^{-5} M (open squares) and 2.95×10^{-5} M (open circles), with $\Delta\epsilon_{11} = -5.0 \times 10^3$ cm⁻¹ M⁻¹, $\Delta\epsilon_{12} = -5.5 \times 10^3$ cm⁻¹ M⁻¹ and $K_{11}(I_c=0) = 4.5 \times 10^{-4}$ M. For K'_{21} , $[An_T] = 7.5 \times 10^{-6}$ M (open diamonds), 1.65×10^{-5} M (crosses) and 2.25×10^{-5} M (solid diamonds). Parameters are as in fig. 2a, with $\Delta\epsilon_{21} = -2.05 \times 10^4$ cm⁻¹ M⁻¹ and $K'_{12} = 1.1 \times 10^{-8}$ M².

Application of eq. (4) to high- $[Ca_T]$ titration points showed that the disproportionation described by reaction (1) above cannot explain the variation of ΔA at high $[Ca_T]$; consequently, some complex, other than $CaAn$, prevails at high Ca concentrations.

The large increase in ΔA at 595 nm (fig. 2a) when $[Ca_T] \geq 10^{-3}$ M is found to be due to progressive stabilization of the complex Ca_2An . Determination of binding and optical parameters was carried out with a somewhat different method than that which was reported previously in parts I and II of this series; the newer method is more sensitive at high Ca concentrations. As before, the general expression for differential absorbance in this system is

$$\Delta A = \Delta\epsilon_{11}[CaAn] + 2\Delta\epsilon_{12}[CaAn_2] + \Delta\epsilon_{21}[Ca_2An], \quad (11)$$

and mass conservation constraints are

$$[Ca_T] = [Ca] + [CaAn] + [CaAn_2] + 2[Ca_2An], \quad (12a)$$

$$[An_T] = [An] + [CaAn] + 2[CaAn_2] + [Ca_2An]. \quad (12b)$$

Solving eq. (11) for $[Ca_2An]$, and inserting the result in eq. (12a) gives the following expression for free Ca:

$$[Ca] = \{ [Ca_T] - 2\Delta A / \Delta\epsilon_{21} \} \times \left\{ 1 + \left(1 - 2 \frac{\Delta\epsilon_{11}}{\Delta\epsilon_{21}} \right) \frac{[An]}{K_{11}} + \left(1 - 4 \frac{\Delta\epsilon_{12}}{\Delta\epsilon_{21}} \right) \frac{[An]^2}{K'_{12}} \right\}^{-1}. \quad (13)$$

Inserting the same value for $[Ca_2An]$ into eq. (12b) transforms the mass conservation law for dye into

$$[An_T] = [An] + \left(1 - \frac{\Delta\epsilon_{11}}{\Delta\epsilon_{21}} \right) \frac{[Ca][An]}{K_{11}} + 2 \left(1 - \frac{\Delta\epsilon_{12}}{\Delta\epsilon_{21}} \right) \frac{[Ca][An]^2}{K'_{12}} + \frac{\Delta A}{\Delta\epsilon_{21}}. \quad (14)$$

For selected values of $\Delta\epsilon_{21}$, $[An]$ was scanned for values in the entire range $0 < [An] < [An_T]$, and that value was found (if any) which satisfied eqs. (13) and (14); the successful set of values ($[An]$, $\Delta\epsilon_{21}$) was then inserted in the expression for K'_{21} :

$$K'_{21} = \{ [Ca]^2 [An] / [Ca_2An] \} \Pi f'_{21} = \{ [Ca]^2 [An] \Pi f'_{21} \} \times \{ [An_T] - [An] - [Ca][An] / K_{11} - 2[Ca][An]^2 / K'_{12} \}^{-1}; \quad (15)$$

in eq. (15), $[Ca_2An]$ has been substituted from eq. (12b) and the definitions of K_{11} and K'_{12} have been inserted for $[CaAn]$ and $[CaAn_2]$.

Optimum constancy for K'_{21} is obtained with $\Delta\epsilon_{21} = -2.05 \times 10^4$ cm⁻¹ M⁻¹ at 595 nm. Analysis of three titration curves is shown in fig. 4 ($\Pi f'_{21} \approx \Pi f_{11}$, as shown in fig. 3, because $CaAn$ is taken to carry no net charge; for the same reason $\Pi f'_{12} \approx \Pi f_{11}$). The overall dissociation equilibrium constant of the complex Ca_2An is found to be 1.5×10^{-6} M².

Table 1

Binding and optical parameters characterizing An complexing with Ca. K'_{pq} values are overall dissociation equilibrium constants for complexes Ca_pAn_q extrapolated to zero ionic strength. Integral extinction coefficients ϵ_{pq} are calculated according to $\epsilon_{pq} = q(\Delta\epsilon_{pq} + \epsilon_{\text{An}})$ (see text); $\epsilon_{\text{An}} = 2.61 \times 10^4 \text{ cm}^{-1} \text{ M}^{-1}$ at 595 nm and $\epsilon_{\text{An}} = 0.3 \times 10^3 \text{ cm}^{-1} \text{ M}^{-1}$ at 710 nm

Complex	K'_{pq}	ϵ_{pq} (595 nm) ($\text{cm}^{-1} \text{ M}^{-1}$)	ϵ_{pq} (710 nm) ($\text{cm}^{-1} \text{ M}^{-1}$)
CaAn	$K_{11} = 4.5 \times 10^{-4} \text{ M}$	$\epsilon_{11} = 2.11 \times 10^4$	$\epsilon_{11} = 8.7 \times 10^3$
CaAn_2	$K'_{12} = 1.1 \times 10^{-8} \text{ M}^2$	$\epsilon_{12} = 4.12 \times 10^4$	$\epsilon_{12} = 2.16 \times 10^4$
Ca_2An	$K'_{21} = 1.5 \times 10^{-6} \text{ M}^2$	$\epsilon_{21} = 5.6 \times 10^3$	$\epsilon_{21} \leq 0.35 \times 10^3$

In brief, complete description of the complexing of An with Ca requires explicit consideration of three different stoichiometric types, CaAn, CaAn_2 and Ca_2An ; the data are summarized in table 1. For a comparison, the identical stoichiometric forms appear in the interaction of arsenazo III with Ca [2], but the greater negative charge of arsenazo III at pH 7.0 lends greater stability to each complex: at zero ionic strength, $K_{11} = 4.5 \times 10^{-4} \text{ M}$ and $K_{11} = 1.6 \times 10^{-6} \text{ M}$ for An and arsenazo III, respectively. The calculated distribu-

tion of An among free and Ca-complexed forms is shown in fig. 5a and b for a low and a high dye concentration.

The titration data at 710 nm corroborated the findings at 595 nm. At 710 nm ΔA is first positive (i.e., Ca-complexed dye has a greater absorbance than does free An), but as $[\text{Ca}_T]$ is increased further the increase in ΔA is reversed, and $\Delta A \approx 0$ at high $[\text{Ca}_T]$ values (cf. fig. 2b). Following the same analytical procedure as above, it was found that also at 710 nm CaAn and CaAn_2 complexing is reflected in the low- $[\text{Ca}_T]$ part of the titration curves. The decline of ΔA at high Ca concentrations was found to reflect formation of the Ca_2An complex, where $\Delta\epsilon_{21} \leq 0.05 \times 10^3 \text{ cm}^{-1} \text{ M}^{-1}$ at 710 nm. The integral extinction coefficients at 710 nm are included in table 1.

4. Antipyrylazo III binds to acetylcholine receptor protein in the presence of Ca^{2+}

In a recent study [3], no evidence of An binding to biological material was evident. Because quantitative evaluation of Ca binding using metallochromic indicators requires knowledge of all binding interactions in the reaction mixture, suitable indicators are only those which are inert with respect to the biological components.

Spectrophotometric Ca titrations of An in the presence of purified acetylcholine receptor protein (AcChR) were performed with the initial aim of determining Ca-binding properties of this protein. Fig. 6 shows the acetylcholine (AcCh) binding isotherm of the purified protein, prepared as described in section 2. The isotherm indicates preservation of the positive cooperativity for AcCh binding which is characteristic of the native mem-

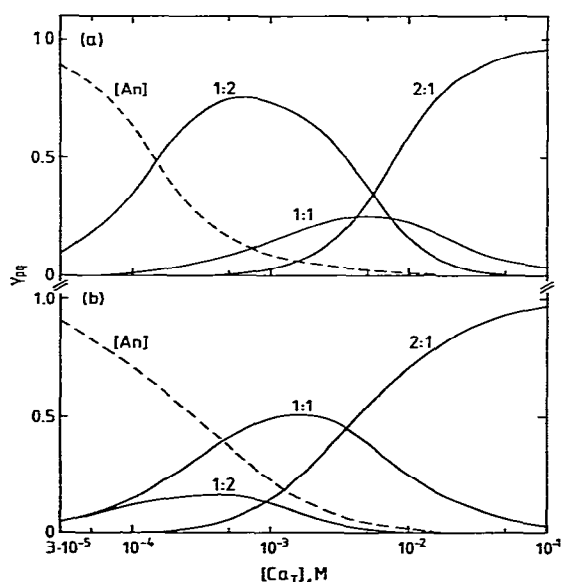


Fig. 5. Calculated fraction of free indicator ($[\text{An}] = [\text{An}]/[\text{An}_T]$) and of indicator bound in the three individual complexes, $p:q$, for a low and a high indicator concentration, respectively: $\gamma_{pq} = q[\text{Ca}_p\text{An}_q]/[\text{An}_T]$. In (a) $[\text{An}_T] = 5.0 \times 10^{-4} \text{ M}$, while in (b) $[\text{An}_T] = 1.0 \times 10^{-5} \text{ M}$.

brane-bound) state, along with retention of high AcCh-affinity sites: $K_{\text{AcCh}} = 4(\pm 1) \times 10^{-9}$ M [8,9].

Fig. 7 compares $\Delta A - [\text{Ca}_T]$ titration curves at the 'Ca-specific' wavelength 710 nm, both in the

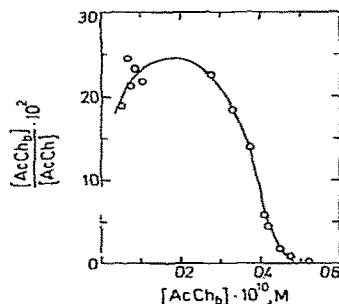


Fig. 6. Binding isotherm of $[^3\text{H}]\text{AcCh}$ with AcChR (13S) at 273 K. The Scatchard plot, i.e., ratio of bound ($[\text{AcCh}_b]$) to free ($[\text{AcCh}]$) AcCh versus $[\text{AcCh}_b]$, indicates positive cooperative binding and retention of high AcCh-affinity binding sites ($K_{\text{AcCh}} \approx 10^{-9}$); see ref. [9].

absence and the presence of AcChR. The binding of dye to protein is immediately evident from the fact that the *maximum* ΔA which is attainable in the presence of protein (cf. the bottom curve in fig. 7) is much smaller than the maximum found in the protein-free case (top curve in fig. 7). Without

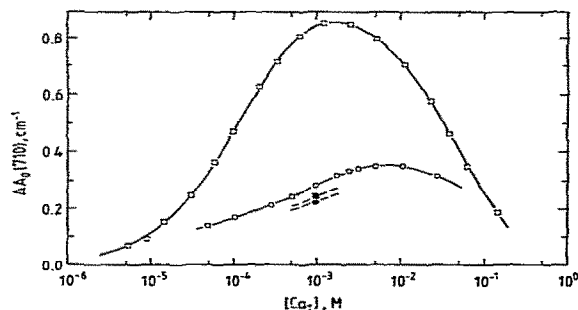


Fig. 7. Spectrophotometric Ca titration of An ($[\text{An}_T] = 1.0 \times 10^{-4}$ M) at 710 nm in the absence (open squares) and presence (open circles) of AcChR (H-form, molecular weight ≈ 500 kd [9]): $[\text{AcChR}_T] = 5.0 \times 10^{-6}$ M, 0.1 M NaCl, 0.1 M Hepes buffer, pH 7.0 at 293 K. Two additional titration points are shown for $[\text{Ca}_T] = 1$ mM: $[\text{AcChR}_T] = 6.0 \times 10^{-6}$ M (solid square) and 7.0×10^{-6} M (solid circle).

protein-dye complexing, $\Delta A - [\text{Ca}_T]$ curves would be only shifted to the right because of Ca binding to the protein and the maximum value of ΔA would remain unchanged. Fig. 7 shows, that with increasing Ca concentration, the amount of An available to Ca^{2+} in solution is less when the protein is present: as shown for $[\text{Ca}_T] = 1$ mM, an increase in protein concentration further decreases the free Ca concentration.

These experimental results present instructive evidence of protein-indicator complexing. The progressive decrease in the absorbance increment with increasing $[\text{Ca}_T]$ indicates that the binding of indicator to protein requires Ca^{2+} . Removal of dye from solution by the protein may therefore be due to the formation of protein-dye-Ca ternary complexes in the form $(\text{AcChR})\text{CaAnCa}$ because $\Delta\epsilon_{21} \ll \Delta\epsilon_{11}$, $\Delta\epsilon_{12}$ at 710 nm. A satisfactory quantitative analysis of this ternary complexation cannot be done, because the physical conditions on the binding interactions, namely, mass conservation laws on dye, Ca and protein, and the law of additive absorptivities, leave the problem undetermined. The data, however, indicate qualitatively that there is appreciable Ca binding to the receptor protein, ranging from the μM to the mM Ca^{2+} -concentration region; this confirms previous results of spectrophotometric titrations with murexide as an indicator [5,6].

5. Titration of acetylcholine receptor protein with acetylcholine

When a solution containing An, Ca and protein is titrated with AcCh, the total absorbance of the mixture at 710 nm increases with increasing AcCh concentration. Three such titration curves, corresponding to three different values of $[\text{Ca}_T]$, are shown in fig. 8. The final value of ΔA is always greater than that in the initial AcCh-free case, suggesting that AcCh binding to receptor protein releases protein-bound Ca^{2+} ; it is seen that $\Delta(\Delta A) = \Delta A(\text{AcCh}) - \Delta A(0)$, where $\Delta A(0)$ corresponds to $[\text{AcCh}] = 0$, is greatest at $[\text{Ca}_T] = 0.5$ mM and least at $[\text{Ca}_T] = 20$ mM. On the other hand, the values of $\Delta(\Delta A)$ are too large to be explained solely by Ca release from protein, and suggest that

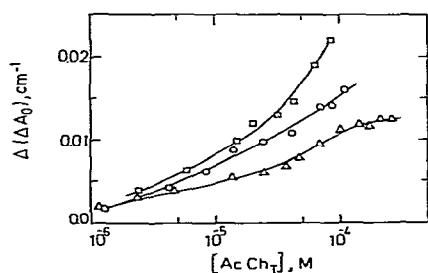


Fig. 8. Spectrophotometric AcCh titration of AcChR: $[AcChR_T] = 8.6 \times 10^{-6}$ M, $[An_T] = 2.0 \times 10^{-4}$ M, 0.1 M NaCl, 0.1 M Hepes, pH 7.0 at 293 K. Relative absorbance increases, $\Delta(\Delta A_0) = \Delta A_0(AcCh) - \Delta A_0(0)$, are consistent with release of Ca^{2+} and indicator upon AcCh binding to the protein: $[Ca_T] = 0.5$ mM (squares), 1.0 mM (circles) and 20 mM (triangles).

AcCh binding releases, in addition, protein-bound indicator molecules. The released indicator molecules revert to $CaAn$ and $CaAn_2$ forms, which are characterized by larger differential absorbance coefficients than is protein-bound indicator. Again, a quantitative analysis is not yet possible.

6. Discussion

Several important differences exist between the determined complexing characteristics of An with Ca and those previously found for the Ca-arsenazo III case. The lesser overall stability of the Ca-An complexes is easily explained in terms of the smaller net negative charge of An. However, the 1:2 Ca-dye complex is more stable relative to the 1:1 complex in the case of An than for arsenazo III: $K_{12}:K_{11} = 2.5 \times 10^{-5} \text{ M}:4.5 \times 10^{-4} \text{ M}$ for An, while the corresponding ratio for arsenazo III was determined to be $3.2 \times 10^{-4} \text{ M}:1.6 \times 10^{-6} \text{ M}$ (at zero ionic strength). The most obvious explanation is that the large excess negative charge of the 1:2 Ca-arsenazo III complex destabilizes this configuration, whereas the positive cooperativity exhibited in $CaAn_2$ formation suggests more stable chelation of the Ca^{2+} by *each* An molecule in the $CaAn_2$ complex than is afforded by 1:1 complexing.

The above-described method for determination of metal-indicator complexing is preferable over

standard graphical techniques, such as Job's method (cf. ref. [10]), the method of normalized slopes [11], double-reciprocal plots and Hill plots. The main advantage of the present method is the allowance for mixing of several stoichiometric types with *different* elementary binding characteristics (previous analyses of metal binding to metallochromic azo indicators have assumed only one type of binding stoichiometry).

Experience with the method showed that the proper sequence for application is to first evaluate the lowest resolvable points on each ΔA - $[Ca_T]$ titration curve, followed thereafter by evaluation of higher ΔA points. In this way, low ΔA values yielded properties of 1:1 and 1:2 Ca-dye complexation, and also showed that the contribution to ΔA at high Ca concentrations is principally due to the 2:1 complex. If, alternatively, the analysis is first applied to higher ΔA values, incorrect conclusions may result: for example, one may find a reasonable fit of the 1:1 complexing model at high $[Ca_T]$ points, but then find that the same parameters fail to cover the data at low calcium concentrations, even if 1:2 complexing is allowed for. The analytical method is most effective if carried out initially for the low- $[Ca_T]$ points of several ΔA - $[Ca_T]$ curves, corresponding to several different dye concentrations, and that combination of binding and optical parameters is found which predicts the same value for K'_{pq} for *every* value of $[An_T]$. In our studies of the Ca-complexing properties of arsenazo III and An, this approach resolved a unique set of parameters for 1:1 and 1:2 Ca-dye complexing, and these parameters were subsequently shown to be optimal in the extended three-complex formalism which resolved the 2:1 parameters.

We find that An binds extensively to AcChR in the presence of Ca, and hence recommend caution in future use of this indicator as a quantitative measure of Ca binding to biological molecules. However, it could be clearly demonstrated with An that the range of Ca-binding to AcChR covers the μM and the mM region. Furthermore, AcCh binding to receptor protein produces a pronounced change in the Ca-binding capacity of the protein, which is most likely due to AcCh-induced conformational changes.

Acknowledgement

We gratefully acknowledge the technical assistance of Ute Santarius, and the financial assistance of the Deutsche Forschungsgemeinschaft, grant Ne 227, the National Institutes of Health, grant 5 RO 1-NS-13744, Muscular Dystrophy Association of America.

References

- [1] P.L. Dorogi and E. Neumann, *Biophys. Chem.* 13 (1981) 117.
- [2] P.L. Dorogi and E. Neumann, *Biophys. Chem.* 13 (1981) 125.
- [3] A. Scarpa, F.J. Brinley and G. Dubyak, *Biochemistry* 17 (1978) 1378.
- [4] A. Scarpa, F.J. Brinley, T. Tiffert and G.R. Dubyak, *Ann. NY Acad. Sci.* 307 (1978) 86.
- [5] H.W. Chang and E. Neumann, *Proc. Natl. Acad. Sci. USA* 73 (1976) 3364.
- [6] E. Neumann and H.W. Chang, *Proc. Natl. Acad. Sci. USA* 73 (1976) 3994.
- [7] N.C. Kendrick, *Anal. Biochem.* 76 (1976) 487.
- [8] H.W. Chang and E. Bock, *Biochemistry* 16 (1977) 4513.
- [9] H.W. Chang and E. Bock, *Biochemistry* 18 (1979) 172.
- [10] Z. Ahmed, L. Kragie and J.A. Connor, *Biophys. J.* 32 (1980) 907.
- [11] M.V. Thomas, *Biophys. J.* 25 (1979) 541.